International Journal of Innovation, Creativity and Change. www.ijicc.net
Volume 15, Issue 3, 2021

Geochemical Proxy of Palaeoclimate of the Pleistocene Coals in Bintuni Basin, West Papua

Ahmad Helman Hamdani[a], Syaiful Alam[b], [a,b,]Faculty of Geology, Universitas Padjadjaran, Jl. Raya Bandung Sumedang Km. 21, Jatinangor, Sumedang, Indonesia 45363, Email: [a*]ahmad.helman@unpad.ac.id, [b]syaiful.alam@unpad.ac.id

The aim of this research is to determine the paleo depositional and palaeoclimatic conditions of coal succession from the Steenkool Formation, Dataran Beimes District, Bintuni Regency, West Papua, Indonesia. The major oxide elements were obtained by X-Ray Fluorescence (XRF) and Laser Ablation Inductively Coupled Plasma-Mass Spectrometry ICP-MS) analyses were used to identify trace element composition. The moderate-to-high value of paleo-weathering parameters such as the Chemical Index of Alteration (CIA), Index of Composition Variable (ICV), a plot of CIA against Al2O3, as well as the Al2O3-CaO+Na2O-K2O Ternary diagram, suggest a moderate-to-strong degree of weathering of the source rocks. The positive correlation between Al2O3 with TiO2, K2O, Fe2O3, and MgO implies that they occur in clay minerals formed from weathering. The palaeoclimatic index (C-value) ranges from 0.47 to 2.06 and low Sr/Ba (0.15–1.22) ratio values, indicating a humid condition during the sedimentation of the coals. The paleo-redox parameters based on Ni/Co, V/Cr and V/(V+Ni) ratios indicate that all the samples were deposited under oxic to anoxic conditions. The coals from Steenkool Formation were deposited in freshwater to low saline water and shows a strong marine influence, due to the alternating salinity and desalinity processes during sedimentation.

Key words: *coal, Steenkool Formation, major oxide, trace element, paleoclimate*

Introduction

Tracking of past climate changes or prediction of future climate change must be done accurately. The methods or tools used need to be clearly understood, so that the interpretation results are completely accurate. One of the methods is the use of rock sequences to track past climate change. As it is impossible to visit the past to ascertain the then-prevalent climate,

researchers use traces of the past to interpret the palaeoclimate, which is called a proxy. Foraminifera, diatoms, coral, spore, density, wood circles and pollen are known to be good climate biological proxies. Other proxies useful in climate determination are the characteristics of sediments such as texture, color and structure, which are indicators of physical proxies. The chemical composition of shells of organisms and sediments are examples of chemical proxies. The coal-forming environment occurs in almost-humid climates worldwide, ranging from the cold Tundra in Canada to the warm tropical swamps of Malaysia, India, Indonesia and part of equatorial Africa (Evelyn, 1999), where geological material was sensitive to hot and wet conditions during coal formation. The worldwide distribution of peat land has led to the common assumption that coal cannot be used for the paleoclimate proxy, due to their broad range over many different climate zones. However, a wide diversity of the wetland zone has occurred. The variety of climatic conditions produces a type of wetland different from bog, fen, and marsh. Further, these wetlands show the specific biological, sedimentological, mineralogical and geochemical properties that allow for the distinct climatic conditions of these wetlands (Seppala, 1988, Finkelman *et al.,* 2019, Dai *al*., 2020).

The geochemical properties of sedimentary rock such as major element, trace element (TE) and rare earth (RRE) are important tools to identify the source provenance, weathering level, tectonic setting and paleoclimate (Rosser *et al.,* 1988, Cox *et al.,* 1995, Fedo *et al*., 1996, Nesbitt *et al*., 1996, Cullers *et al.,* 2000). The paleo redox of sedimentary rock can be used to deduce geochemical parameters (Dypvic, 1984, Culler, 2002, Rimmer, 2004).

The Steenkool Formation consists of inter-bedded quartz sandstone, mudstone, shale, and coal, deposited in the Bintuni Basin, West Papua. During the Pliocene to Pleistocene periods, in the NE of the basin, prograding fluvio-deltaic to paralic was commonly deposited in this formation (Djadjang *et al,* 2018). While in the southern part, the formation was deposited in Early Low Stand Wedge to Late Low Stand Wedge Submarine Fan (Nugrahanto *et al*.,2001, Alam and Djadjang, 2019).

Based on the pollen assemblages in sediment, repeated glacial and inter-glacial periods associated with various conditions such as warm, dry and wet climates were the conditions in Papua Island during the Pleistocene epoch (Lelono, 2017). It is very interesting to study climate change in Papua through the composition of major oxide and trace elements within coal in the Steenkool Formation. Therefore, the Steenkool Formation poses a scientific challenge to the research of chemical proxies in tracking climate change during the Pleistocene epoch in Papua.

The aims of this study were to determine the depositional environment, including the redox conditions, palaeosalinity, and palaeoclimate conditions during the deposition of coal in the Steenkool Formation, by examining chemical proxies. This study contributes to the understanding of the Pliocene-Pleistocene paleoclimate change.

Geological Setting

Geologically, the research area was located in the Northeastern Part of Bintuni Basin. The Bintuni Basin is one of the sedimentary basins located in the West Papua region. This basin is well known as a Tertiary basin that produces large hydrocarbons in the Eastern part of Indonesia; one of them is Tangguh Gas Field.

The boundaries of Bintuni Basin (Figure 1A); the eastern part of the basin region is bounded by Lengguru Fold-Thrust Belt (Babault, J., et al. 2018), the northern part is bounded by the oldest rock of Kemum Block and Ayamaru Plateau, the western part is bounded by Misool-Onin-Kumawa structural High (Putra and Husein, S., 2019), and the southern part is bounded by Tarera- Aiduna Fault

The stratigraphic sequence in the Northeastern part of the Bintuni Basin includes the Klasafet Formation, the Steenkool Formation, and the Sele Formation (Figure 1B). The oldest rock units that fill the Bintuni Basin are known as the Klasafet Formation. As described by Pieters et al. (1990), the unit is composed of marl, lime-stone mudstone, and shale with a small insertion of limestone sandstone, calcarenite, and calcirudite. In some sections, a small number of limestone conglomerate inserts were also found. The rock group is believed to have been deposited in an open ocean exposure environment that developed near carbonate deposits. The Steenkool Formation, which is the main deposit in the Bintuni Basin, which is composed of sandstones, mudstones, siltstone and conglomerates with calcarenite and coal deposits. Based on the dominance of the constituent lithology types, Pieters *et al* (1990) divided the Steenkool Formation into two "members", namely the Sandstone Member (TQss), which is dominated by sandstone and the Mudstone Member" which is dominated by mudstone (TQsm). The rocks that make up this unit are interpreted as deposits that form in environments ranging from deltaic to paralic environments.

Figure 1. Location, Simplified Tectonic Element Maps and regional stratigraphy of the Bird's Head of Papua (Source: Nugrohanto *et al*., 2001; Sapiie *et al*, 2012).

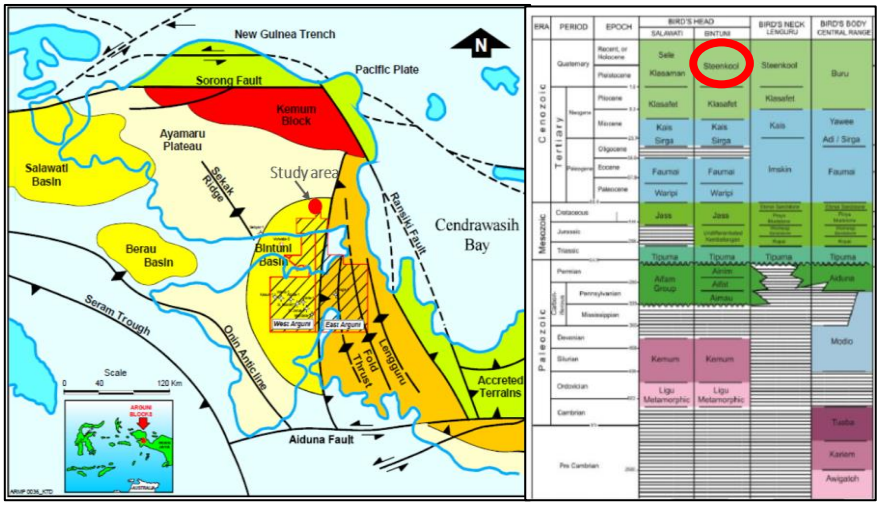

Research Methodology

Coal Sampling

A total of eighteen coal samples were obtained from nine coal seams of the Steenkool Formation. In this study, coals obtained from systematically geological section A-B including coal seam A to I were collected as samples for geochemical element analyses (Figure 2).

Figure 2. Stratigraphy section of Section A-B, showing the succession of lithology and coal seam from Steenkool Formation (left). The Geological Map of the study area (right). The coal seam A to I were subject to geochemical analyses.

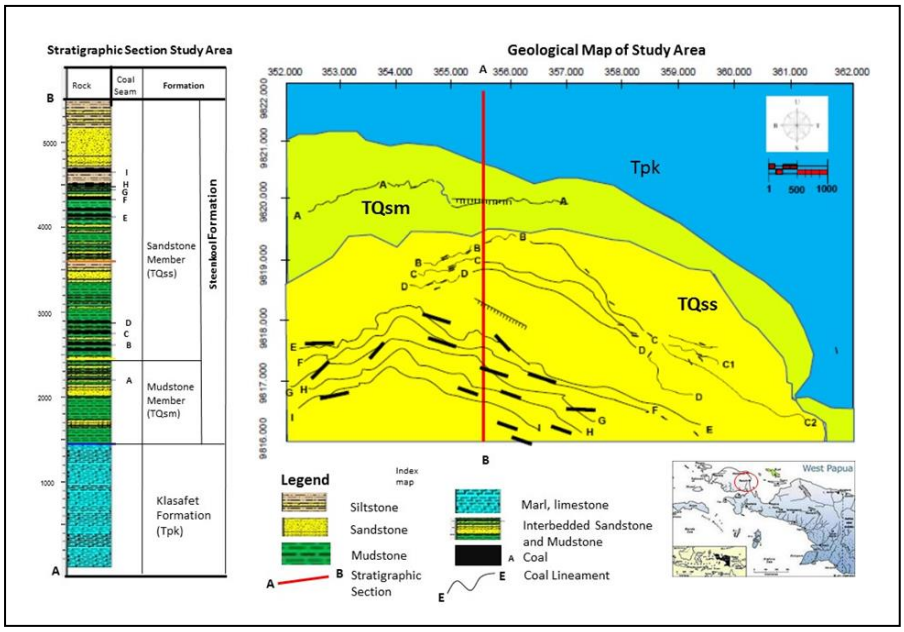

Analytical Procedure

The coal sampling procedures are depicted in Figure 2. Stratigraphy section of Section A-B, shows the succession of lithology and coal seam from Steenkool Formation (left), while the geological map of the study area is on the right. The coal seams A to I were subjected to geochemical analyses.

The preparation and bagging in the study are according to the ASTM International Standard. To avoid and reduce contamination exfiltration and weathering, coal samples were put in a resealable polyethylene plastic bag. The coal was air dried and crushed until it is fine enough to pass through a 200-mesh sieve. It was then divided into representative amounts for chemical analysis. Coal powder sample was acid-digested with a combination of HNO3, HCl, HF in the ratio of 3:1:1 respectively. Further, separation of the ash concentration was carried out by heating to a temperature of 8150 C following the ASTM standard procedure; the ash obtained was analysed using XRF on fused glass beads in the Sucofindo, Indonesia, to determine the

composition of the major oxide. The major oxides i.e.: SIO_2, Al_2O_3, Fe_2O_3, CaO, MgO, K_2O, MgO, MgO, MnO, Na_2O, TiO_2 and LOI were calculated in percentage weight. The selective trace elements were identified by the ICP-MS and reported as trace elements. For the comparison of major oxide and trace elements, we used PAAS (Post-Archean Australian Shale) values (Taylor and McLennan, 1985, Condie, 1993). The Enrichment Factor (EF) was used to determine the degree of enrichment of trace elements in the sediment, as it has been widely used universally (Calvert, and Pedersen, 1993; Ross and Bustin, 2009). Enrichment Factor (EF) was calculated by normalising each element against aluminum (Al), and comparing the ratio with its equivalent in normal shale, such as the average value in shale (e.g. PAAS) (Rimmer, 2004)

Result

Major Oxide

The analysis of major oxide composition in the eighteen coals is seen in Table 1. Trace Element data are tabulated in Table 2. The elements of Si, Al, Fe, Ca and Mg were abundant in coal samples; therefore, K, Na, Ti, Mn and P were lo (content below 1 %).

Table 1. Major Oxide composition of coals from the Steenkool Formation

Coal Seam	SiO_2	Al_2O_3	Fe_2O_3	MnO	MgO	CaO	Na_2O	K_2O	TiO_2	P_2O_5	CIA	ICV
	(%)											
Mudstone Member (TQsm)												
A	49.45	14.12	5.61	0.61	0.08	7.21	9.21	0.82	0.83	0.31	61.44	1.73
A	42.41	11.15	4.73	0.73	0.03	6.13	3.24	1.79	1.64	0.06	51.36	1.73
A	46.59	12.14	5.79	0.79	0.01	5.96	4.76	1.79	0.35	0.44	59.98	1.60
A	48.46	13.43	6.84	0.38	0.02	8.02	8.18	0.55	0.42	0.11	59.90	1.82
A	42.25	14.83	5.28	1.28	0.02	7.18	7.73	0.91	0.31	0.07	63.84	1.53
Sandstone Member (TQss)												
B	27.57	10.25	30.19	0.59	0.02	7.66	8.88	0.26	0.87	0.04	53.83	4.73
B	32.17	12.81	30.57	0.57	0.03	4.66	8.09	1.17	0.84	0.05	65.76	3.59
C	25.61	11.67	29.13	0.62	0.02	7.99	9.59	0.32	0.89	0.04	55.92	4.16
C	25.15	12.32	23.11	0.71	0.03	8.19	10.21	0.31	0.91	0.05	56.70	3.53
D	29.45	10.12	21.12	0.61	0.08	6.21	14.21	0.82	0.83	0.31	56.28	4.34
D	25.65	14.86	15.73	0.57	0.04	10.17	11.26	0.74	0.97	0.43	55.57	2.66
E	40.45	20.15	9.8	0.73	0.03	6.13	7.24	2.79	1.64	0.06	65.61	1.41
E	46.59	26.14	7.85	0.79	0.01	3.96	4.76	1.79	0.35	0.44	81.08	0.75
E	48.46	21.43	14.86	0.38	0.02	4.02	2.18	0.55	0.42	0.11	81.11	1.05
F	48.97	24.14	8.07	0.63	0.04	3.14	4.98	2.33	0.06	0.04	81.36	0.80
G	48.97	26.13	7.34	0.57	0.08	1.24	5.31	3.14	0.34	0.07	84.42	0.69
H	50.48	23.26	7.28	0.51	0.07	2.65	3.59	2.52	0.31	0.07	80.93	0.73

I	50.59	22.18	8.87	0.59	0.09	2.01	0.91	2.18	0.62	0.11	82.18	0.75
Max	50.59	26.14	30.57	0.79	0.09	10.17	14.21	3.14	1.64	0.44	84.42	4.73
Min	25.15	10.12	7.28	0.38	0.01	1.24	0.91	0.26	0.06	0.04	53.83	0.69
Average	38.47	18.11	16.46	0.61	0.04	5.23	7.02	1.19	0.70	0.14	69.29	2.24
PASS	62.80	19.00	6.50	1.00	0.10	1.30	2.2	1.7	1.20	0.22		

CIA: Chemical Index Alteration; ICV = Index Compositional Variability

In Mudstone Member (TQsm), only one coal seam was identified (coal seam A), while in Sandstone Member (TQss), nine coal seams were identified, named seam B, C, D, E, F, G, H and I. The abundance of major oxide in the Steenkool Formation can be divided into three groups, viz., SiO2, Al2O3 and Fe2O3; Ca and MgO and MnO2, TiO2, N2O, K2O,and P2O5. Figure 3 shows the bivariate plot of major oxide composition to PAAS (Taylor and McLennan, 1985). Figure 3. The bivariate plot of major oxide composition to PAAS (after Taylor and McLennan, 1985) of the coal from the Mudstone Member (TQsm) and the Sandstone Member (TQss).

Figure 3. The bivariate plot of major oxide composition relative to PAAS of the Mudstone Member (left) and Sandstone Member (right).

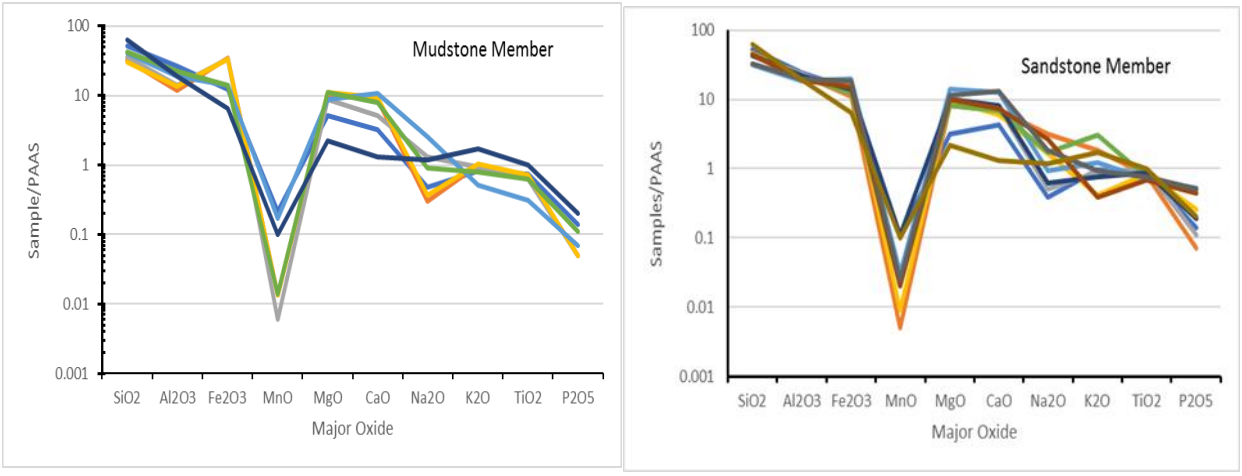

The coals show the main major element oxide as SiO_2; Al_2O_3, and Fe_2O_3); only SiO_2 was depleted relative to PAAS both in Mudstone Member and Sandstone Member of the Steenkool Formation (Figure 3). The depleted SiO_2 relative to PAAS reflected the lowest quartz minerals in sediments related to the chemical weathering in the parent area. The analysis of major oxide in all samples showed a moderate quantum of SiO_2 and low abundances of K_2O (Potassium feldspar) and N_2O (Sodium feldspar), reflecting weathering of the parent rock. The low content of K_2O (below 1 wt. %) indicates a strong level of chemical weathering.

The significant enrichment of Al_2O_3 in coals suggested that the presence of high Al-bearing minerals, such as shale and/or clay components is due to the strong chemical weathering of the original rocks. The enrichment of Fe_2O_3 reflected the high concentration of non-silicate minerals (such as hematite) within sediments. Other oxides such as MnO, Na_2O, K_2O, TiO_2, and P_2O_5 were depleted compared to the PAAS values, while CaO and MgO were enriched, vis-a-vis the PAAS values. The strong chemical weathering of the original rock causes the loss of feldspar minerals, characterised by depletion of Na_2O and K_2O, also supported by the greater proportion of clay minerals (especially kaolinite) in the coals.

Trace Element in Coal Samples from Steenkool Formation

The composition and ratio of the trace elements of the coal of Steenkool Formation, both TQsm and TQss, was tabulated (Table 2 and Table 3). This table also shows that, on an average, the most abundant trace element in coal samples was as follows: Ba (average 526.29 ppm), and Sr (204 ppm), followed in abundance by V (average 118.67 ppm). Other trace element content was below 100 ppm.

Besides this, the table also contains the EF for trace elements: B (EF=1.19) and Sr (EF= 1.02) are enriched, while V (EF=0.50), Cr (EF=0.17), Co (EF=0.24), Ni (EF=0.98), and Ba (EF=0.81) are depleted relative to PAAS.

Table 2. Trace element composition in coals from Steenkool Formation

Coal Seam	B (ppm)	V (ppm)	Cr (ppm)	Co (ppm)	Ni (ppm)	Sr ppm)	Ba (ppm)	C Value	SP
Mudstone Member (TQsm)									
A	132	15.00	16.1	14.6	22.2	326.3	514	0.56	77.47
A	128	32.12	17.6	13.1	19	65.3	847	0.54	12.15
A	118	30.24	19	13.8	18.7	59.1	707	0.65	23.10
A	121	29.41	17.2	14.5	21.5	227.1	468	0.48	99.79
A	106	121.88	18.7	14.3	22.9	126.2	710	0.48	48.81
Sandstone Member (TQss)									
B	110	62.60	15.8	14.4	21.2	352	415	0.68	199.33
B	120	71.30	17.7	15	21.2	358	523	0.55	41.71
C	120	75.20	17.6	15.1	20.3	421.4	637	1.70	175.78
C	160	81.28	24.7	16.8	20.8	468.1	847	2.06	244.73
D	120	64.21	18.9	12	18	369.1	707	1.55	63.50
D	121	126.00	18.3	13	16.7	117.1	488	1.17	71.98
E	106	129.34	17.4	13.1	18.4	104.6	300	0.96	8.30
E	110	136.23	18.8	10.73	15.1	208.5	302	0.72	20.91
E	115	104.23	20.2	10.61	14.3	114.6	421	2.06	94.46

F	120	119.21	18	11.56	16.7	198.5	358	0.77	15.43
G	105	48.12	17.6	11.1	14.3	42.9	387	0.64	5.67
H	116	45.21	19.5	14.9	18.2	72.5	426	0.59	12.54
I	108	54.11	16.8	11.2	14.8	51.4	416	0.69	14.64
Max	160	136.23	24.7	16.8	22.9	468.1	847		
Min	105	15	15.8	10.61	14.3	42.9	300		
Average	118.67	74.76	18.33	13.32	18.57	204.59	526.29		
PAAS	100	150	110	55	19	200	650		
EF	1.19	0.50	0.17	0.24	0.98	1.02	0.81		

SP: palaeosalinity; EF: enrichment factors

Table 3. Ratio of trace element in coals from Steenkool Formation

Coal Seam	V/(V+Ni)	V/Cr	Cr/Ni	Ni/Co	Sr/Ba
A	0.40	0.93	0.73	1.52	0.63
A	0.63	1.83	0.93	1.45	0.077
A	0.62	1.59	1.02	1.36	0.084
A	0.58	1.71	0.80	1.48	0.49
A	0.84	6.52	0.82	1.60	0.18
B	0.75	3.96	0.75	1.47	0.85
B	0.77	4.03	0.83	1.41	0.68
C	0.79	4.27	0.87	1.34	0.66
C	0.80	3.29	1.19	1.24	0.55
D	0.78	3.40	1.05	1.50	0.52
D	0.88	6.89	1.10	1.28	0.24
E	0.88	7.43	0.95	1.40	0.35
E	0.90	7.25	1.25	1.41	0.69
E	0.88	5.16	1.41	1.35	0.27
F	0.88	6.62	1.08	1.44	0.55
G	0.77	2.73	1.23	1.29	0.11
H	0.71	2.32	1.07	1.22	0.17
I	0.79	3.22	1.14	1.32	0.12
Max	0.90	7.43	1.41	1.60	0.85
Min	0.40	0.93	0.73	1.22	0.08
Average	0.76	4.06	1.01	1.39	0.40

Discussion

Palaeoweathering Source Area

To determine the level of weathering in the original rock area, the CIA (Chemical Index of Alteration) is used (Nesbitt and Young, 1982).

$$CIA=100\times[Al2O3/(Al2O3+CaO^{*}+Na2O+K2O)] \quad (1)$$

CaO * is the content of calcium oxide in the silicate fraction. To determine the value of CaO, the indirect method, calculating the difference between the total molar proportions of CaO minus the molar proportion of P_2O_5. If the difference is smaller than the mole fraction of Na_2O, the mole difference present is considered as the Cao proportion of the silicate fraction; however, if the difference is greater than the Na_2O fraction, then the number of moles of Na_2O becomes the molar proportion of CaO in the silicate fraction.

Plotting CIA data of all coals on the Al_2O_3-CaO + Na_2O-K_20 triangle diagram (Figure 4) shows that coal from TQsm show weak weathering (average CIA value 59.13) and the overlying TQss indicate more intense weathering (the average CIA value: 69.29).

Figure 4. Triangular A–CN–K diagram with CIA values with vertical axis for the coal from Steenkool Formation are represented by the red circle.

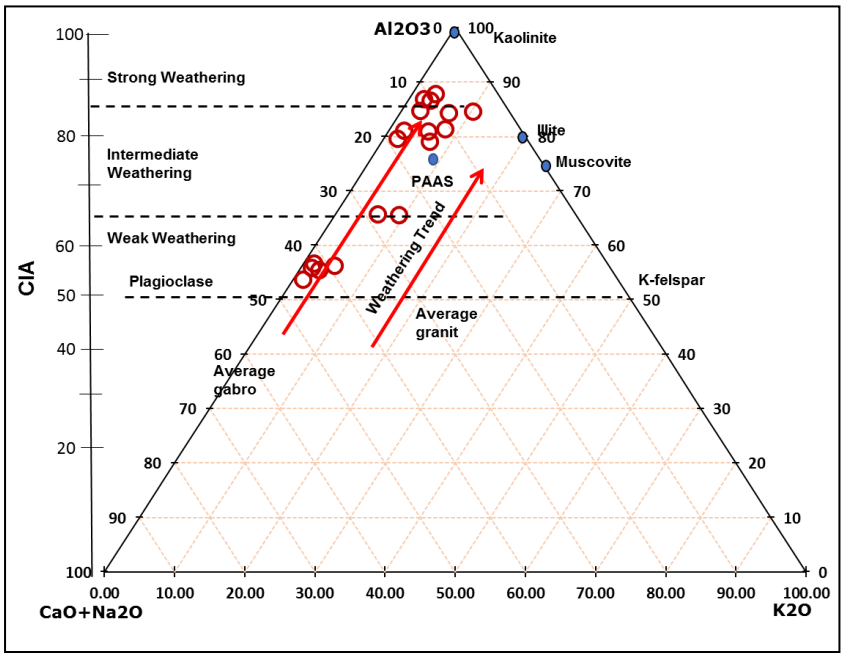

Palaeodepositional from Geochemical Proxies

Trace elements and the ratio of these elements can be used as proxies to determine the current and past depositional environments; such as for example to determine temperature and precipitation (Sheldon *et al*., 2002; Sheldon *et al*., 2006); palaeosalinty (Dypvik, 1984, Hatch and Leventhal, 1992) and redox conditions (Jones and Manning, 1994).

Palaeoclimate

Sheldon *et al*., (2002, 2006) deduce palaeo-precipitation and palaeo-temperature based on the data base of major element of modern soil; which show that the degree of chemical weathering in soils increases with mean annual precipitation (MAP) and mean annual temperature (MAT).

$$MAP = 14.26\ (CIA\text{-}K) - 37.632\ (mm/year) \quad (2)$$

$$CIA - K = 100 \times [Al_2O_3/\ (Al_2O_3 + CaO + Na_2O)] \quad (3)$$

$$MAT = 46.94\ C + 3.99\ (^0\ C) \quad (4)$$

Where: CIA : Chemical Index Alteration

C : mA/mSi (m is the molar ratio)

The MAP results of TQsm obtained from Equation 1 ranged from 803.04 mm/year (average 864.77 mm/year), and in TQss, increased from 740.94 to 1307.53 mm/year with an average of 1004, 70 mm/year. The temperature result obtained from Equation 4 showed a similar trend of MAP; in the TQsm, the temperatures were low (10.91 – 13.32^0 C; average 11.63^0 C), while in the TQss, the temperatures ranged from 13.12^0 C to 19.38^0 C (average 16.39^0 C). Based on the climofunction (Sheldon, 2006), the climate during the formation of Steenkool Formation was humid and warm.

Considering the trend of alignment of element association with climatic conditions, the elements Cr, Mn, Fe, Ni, Co, and V tend to concentrate in humid or moist climates, while in arid climates, due to the nature of water alkalinity related to evaporation, other elements such as Ba, Mg, Ca, Na, K and Sr are enriched. The comparisons between trace element groups can be used as a proxy for climate, which is called the C-value (Cao *et al*., 2012). The equation of the C-value is:

$$\text{C-value} : \sum (Fe+Mn+Cr+Ni+V+Co)/\sum(Ca+Mg+Sr+Ba+K+Na) \quad (5)$$

In our study, the C-value of the coals from the C-value in TQsm was lower than the C-value of TQss (Table 2). The low C-value in TQsm (0.47-0.65, average 0.54) indicated that the palaeoclimatic condition was semi-arid to semi-moist – semi moist (Figure 5A, Hu, *et al*., 2016) or arid to humid (Figure 5C; Liang *et al*., 2020). The C-value in TQss was higher (> 1.0), between 0.54 – 2.6 with an average of 1.14; it is suggested that semi-arid to moist ((Figure 5B, after Hu, *et al*., 2016)) or arid to humid (Figure 5D; Liang *et al*., 2020) conditions influenced the formation of coals.

Figure 5. The C-value (Σ(Fe+Mn+Cr+Ni+V+Co)/Σ(Ca+Mg+Sr+Ba+K+Na)) of the coal samples, reflecting paleoclimate. The discriminating criteria of C-Value (A, C after Hu, et al. 2016), and (B, D after Liang et al., 2020).

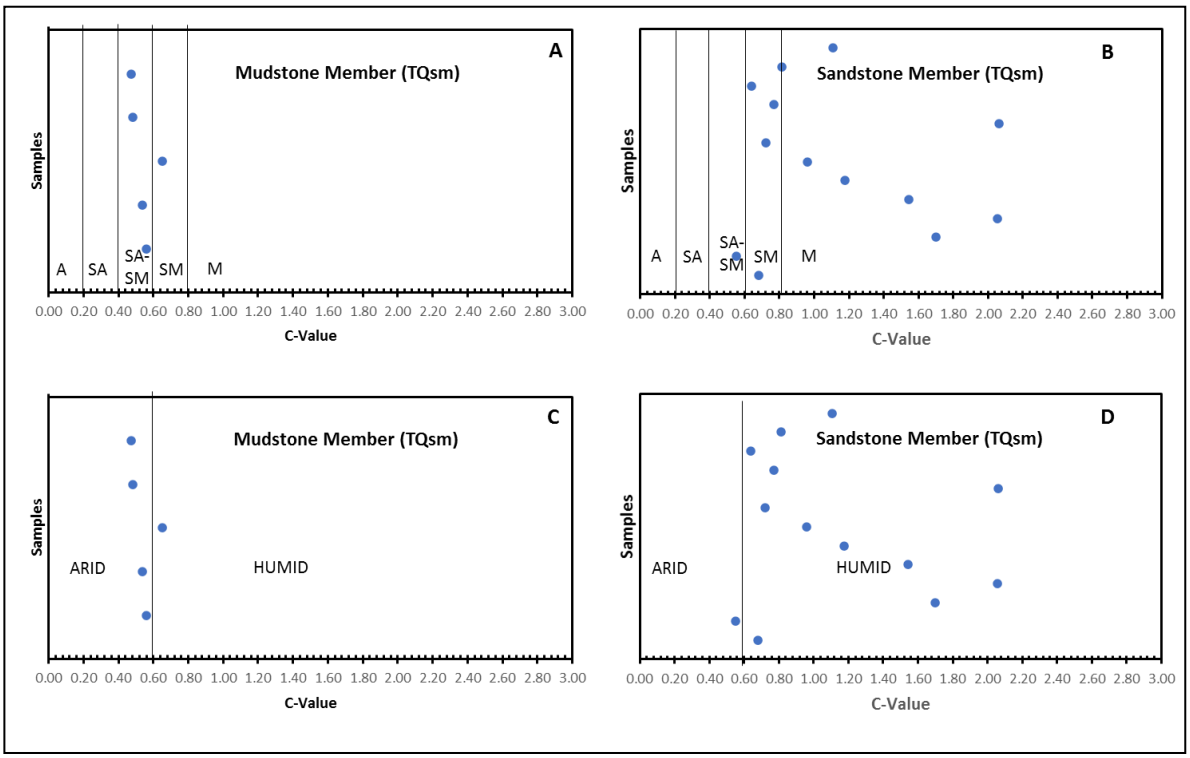

Palaeosalinity reconstruction

The Sr / Ba The Sr / Ba ratio was used as a proxy for palaeoclimate, based on the characteristic that naturally, the Sr element migrates more easily than Ba in aqueous solutions. In addition, it is known that in the organic fraction, clay minerals absorb Sr easily. Based on the data of modern fresh water, brackish water and seawater or modern sediment, the content of Sr and Ba shows a significant difference. The fresh water exhibits a median value of Sr and Ba at 79 and 427 ppm, respectively. Modern brackish water shows a median of Sr and Ba at 182 ppm and 391 ppm respectively. The median of Sr and Ba at 160 ppm and 404 ppm respectively is mostly found in the modern marine sediment. Therefore, the Sr / Ba ratio can be used to determine the variation of salinity in the water column from fresh water to marine sediment, corresponding to climate change.

In our study, the Sr/Ba values of coal samples from TQsm ranged between 0.07 to 0.63 and those from TQss, between 0.11 – 0.85 (Table 3). Based on this ratio, the succession during coal sedimentation was high-low-high (in TQsm) and following high-to-low (Figure 6), reflecting the change of salinity of the water column. The salinity facies of coal succession in Steenkool Formation are Sr/Ba < 0.2 fresh; Sr/Ba 0-2 - 0.5 which is brackish, and Sr/Ba > 0.5 marine environment. The Sr/Ba ratio also indicated that salinity was experienced during the coal sedimentation and de-salinity alternation process during regression.

Figure 6. Bivariate plot of Strontium-barium in coals of Steenkool Formation: (Left) distribution coal samples of Mudstone Member (TQsm) and (Right) distribution coal samples of Sandstone Member (TQss). The thresholds between salinity facies are shown as blue diagonal lines.

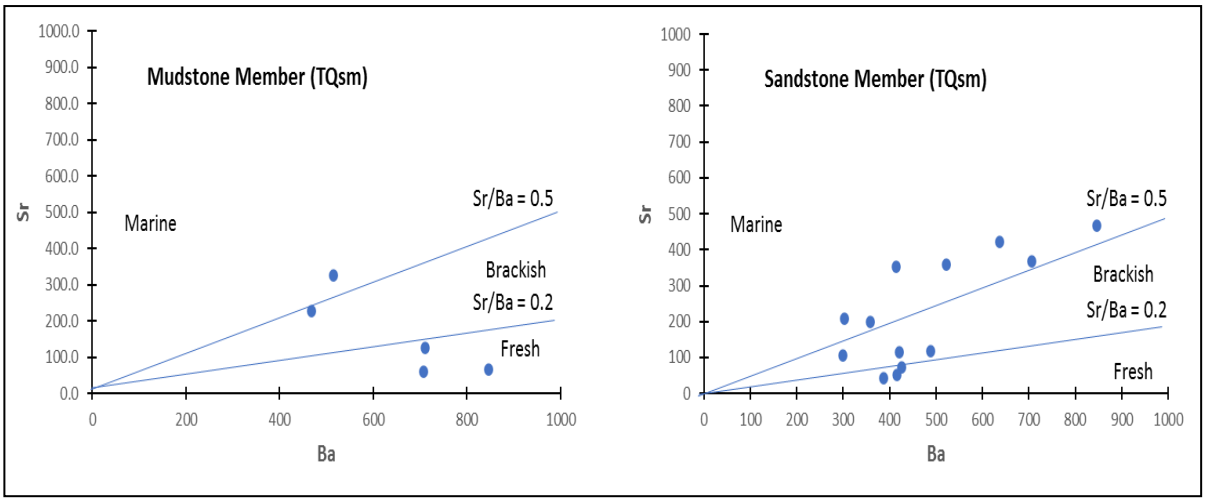

Goldschmidt and Peter in early 1932 and Jones and Manning in 1994 mentioned the use of Boron (B) as a palaeo-salinity proxy for argillaceous sediments. The B content in fresh water was lower (2 ppm) compared to marine waters (20-50 ppm), as mentioned by Couch (1971). Ji et al. (2006) also found that B content in marine shale was higher than the B in the fresh-water shale. Retallac (2020) showed that the B / K ratio >40 µg/g can be used to distinguish marine and non-marine environments (rivers, lakes) (Nussman, 1966, Chetelat et al., 2009, Xi et al., 2011). To determine palaeo-salinity (SP), Adam's formula can be used by performing the adjusted Boron and calculated Boron equivalence (Xiaochunet al., 2020).

$$\text{Adjusted boron} = B \times (8.5/K_2O\ (\%)) \quad (6)$$

$$\text{Equivalent Boron (EBC)} = 11.8 \times (\text{Adjusted Boron}/1.7 \times (11.8\text{-}K_{2=O}) \quad (7)$$

$$SP = 0.0977\ X - 7.043 \quad (8)$$

Where SP is the palaeo-salinity (%) and X is Walker; s Walker's EBC

In this study, the result of palaeo-salinity (SP) of coals from TQsm ranged between 12.20 and 99.79, which belongs to the range of mid-salt water to super-saline water. Similarly, the TQss ranged between 5.67 and 199.33 (Table 2). These results indicate an agreement with the Sr /Ba ratio, reflecting the presence of alternating processes of salinity and de-salinity during the coal formation process.

Palaeoredox Condition

Analysis of trace element composition in the coal of the Steenkool Formation has been used to determine the redox conditions. Several trace elements such as Cr, Ni, V, M, U and Cr are

highly sensitive and tend to be less soluble under reducing conditions, but more soluble under oxidizing conditions (Michael *et al*., 2019).

Based on the V / Cr ratio (Jones and Manning, 1994) redox conditions can be grouped into oxic conditions (V / Cr: <2), dysoxic conditions (V / Cr: 2-4.25) and suboxic to anoxic conditions (V / Cr:> 4.25). A comparison between the elements nickel and cobalt (Ni / Co) was also proposed by Jones and Manning (1994) as a redox indicator. The oxic state has a Ni / Co value smaller than 5, whereas Ni / Co values between 5 and 7 indicate dysoxic conditions; and suboxic to anoxic conditions are characterised by a Ni / Co value greater than 7. Hatch and Leventhal (1992) proposed a comparison between the elements vanadium and Nickel; V / (V + Ni) is used to distinguish redox conditions; dysoxic conditions characterized were by V / (V + Ni) values ranging from 0.46 - 0.50 and anoxic conditions by the value of V / (V + Ni) ranging from 0.54–0.82; and a V / (V + Ni) value greater than 0.84 characterises the euxinic condition

Table 3 shows the range of the V/(V+Ni) between 0.40 to 0.84 with an average of 0.61 in TQs min TQsm, reflecting an anoxic waters environment, while in TQss, the range is higher than in TQsm; i.e. 0.75 to 90 (average 0.81) indicating anoxic to euxinic conditions. The Ni/Co ratio values of the TQsm coal ranged from 1.36 to 1.60 with an average of 1.48, while TQss had relative similar Ni/Co ratio (the average 1.36) due to low value of Ni/Co below 5; it is suggested that an oxic environment influenced TQsm and TQss. The V/Cr ratio value in TQsm ranged between 0.93 – 6.52 with average 2.52, suggesting dysoxic to suboxic conditions. In the TQss, the V/Cr ratio had an average value 4.66, indicating suboxic to anoxic conditions. In this study, we found an inconsistency between redox indicators, as seen from Ni/Co ratio fall in values indicating an oxic environment, while the V/Cr and V/(V+Ni) ratio values indicated a more anoxic environment. The emergence of differences between these redox parameters indicates that the redox parameter is controlled by various factors involving provenance, and these parameters must be used with caution.

Conclusion

Research on the composition of major oxide and trace elements in the Steenkool coal formation in the Bintuni Basin was carried out in an effort to determine the depositional conditions and palaeoclimate. Based on the Chemical Index of Alteration values ranging from 53.83-86.67, it was concluded that there was weak to moderate weathering in the original rock area. Oxic to anoxic conditions characterised by a low average Ni / Co ratio (1.39) and a moderate V / Cr value (3.98) were the redox conditions at the time of coal formation. The low-to-moderate and to high palaeosalinity values based on Adam's value (0.83 -244.73) and Sr/Ba ratio values indicate a fresh water - brackish water and marine water environment coals sedimentation, pointing to the alternating salinity and de-salinity during coal formation. The palaeoclimate indexes such as C-value (0.56–2.06) indicate an arid-to-humid climatic condition. The cold arid climate of the Mudstone Member (TQsm) was characterised by a relatively low CIA, depleted in Fe_2O_3 and Al2O3. The climate condition in the Sandstone Member (TQsm) was warm and

humid, as indicated by the relatively moderate CIA values (55.92-82,18), enrichment of Al_2O_3 and low $K2O/Al_2O_3$. The distinct difference in major oxide composition of coals in the Mudstone Member (TQsm) and Sandstone Member (TQss) are due to climate change during deposition.

Acknowledgements

The authors are grateful to the funding from the University Padjadjaran Research Programme of the Academic Leadership Grant (ALG) of the year 2020. The authors also would like to acknowledge the Dean of Faculty of Geology for their support to establish this article.

Conflicts of Interest

"The author(s) declare(s) that there are no conflicts of interest regarding the publication of this paper."

REFERENCES

Alam S, and Djadjang S. (2019). Tertiary Sequence Stratigraphy of Bird Head Area, Eastern Indonesia, *Indonesian Journal on Geoscience*, 6 (3): 267-278.

Babault, J. (2018). Source-to-sink constraints on tectonic and sedimentary evolution of the western Central Range and Cendrawasih Bay (Indonesia), *Journal of Asian Earth Sciences*, 156. 265-287.

Calvert, S.E and Pedersen, T.F. (1993). Geochemistry of Recent oxic and anoxic marine sediments: Implications for the geological record. *Marine Geol*ogy., 113, 67–88

Cao, J., Wu, M., Chen, Y., Hu, K., Bian, L., Wang, L. and Zhang, Y. (2012). Trace and rare earth element geochemistry of Jurassic mudstones in the northern Qaidam Basin, northwest China. *Chemie der Erde*, 72(3), 245-252.

Chetelat, B., Liu, C. Q., Gaillardet, J., Wang, Q. L., Zhao, Z. Q., Liang, C. S., Xiao, Y. K. (2009). Boron isotope geochemistry of the Changjiang basin rivers, *Geochim. Cosmochim, Acta*, 73, 6084-6097

Couch, E.L. (1971). Calculation of palaeosalinities from boron and clay minerals data. *AAPG, Bull*.,55, 1829-1837

Condie, K. C. (1993). Chemical composition and evolution of the upper continental crust: contrasting results from surface samples and shales, *Chemical Geology*, 104, 1-37,

Cox, R, Lowe, D. R, and Cullers R. L. (1995). The influence of sediment recycling and basement composition on evolution of mudrock chemistry in the southwestern United States, *Geochimica et Cosmochimica Acta*, 59 (14), 2919-2940

Cullers R.L and Podkovyro V.N. (2000). Geochemistry of the Mesoproterozoic Lakhanda shales in southeastern Yakutia, Russia: Implications for mineralogical and provenance control, and recycling, *J Precambrian Research*, 10, 77–93.

Cullers R. L. (2002). Implications of elemental concentrations for provenance, redox conditions, and metamorphic studies of shale and limestones ne Pueblo, CO, USA, *Chemical. Geology*, 191: 305.

Dai S., Bechtelc A., Cortland F.E., Romeo M.F., David F.T., Graham I. T., Madison M.H., James C.H., Vera A.K, Tim A., O'Keefe J. M. K. (2020). Recognition of peat depositional environments in coal: A review. *International Journal of Coal Geology*. 219, 1-67.

Djadjang S, Alam S, Nurdrajat, Muljana B,. Gani R. M. G, Firmansyah Y. (2018). Batubara Formasi Steekool Di Daerah Ransiki, Papua. *Bulletin of Scientific Contribution: GEOLOGY*, 16 (3), 237-246.

Dypvik, H. (1984) Geochemical Compositions and Depositional Conditions of Upper Jurassic and Lower Cretaceous Yorkshire Clays, *England. Geol. Mag*. 12, 489–504.

Dai S., Bechtelc A., Cortland F.E., Romeo M.F., David F.T., Graham I. T., Madison M.H., James C.H., Vera A.K.. Tim A., O'Keefe J. M. K. (2020). Recognition of peat depositional environments in coal: A review. *International Journal of Coal Geology*. 219, 1-67.

Ericson, D.B., Ewing, M., Wollin, G., Heezen, B.C., (1961). Atlantic deep-sea sediment cores. *Geol. Soc. Amer. Bull*. 72, 193–286

Evelyn S. K. (1999). Permian palsa mires as paleoenvironmental proxies, *Palaios* 14 (6),530–544

Farquhar, S.M., Pearce, J.K., Dawson, G.K.W., Golab, A., Sommacal, S., Kirste, D., Biddle, D., Golding, S.D. (2014). A fresh approach to investigating CO2 storage: Experimental CO2-water-rock interactions in a low-salinity reservoir system, *Chemical Geology*, 1-70.

Fedo C.M, Eriksson K, Krogstad, E.J. (1996). Geochemistry of shale from the Archean (~3.0 Ga) Buhwa Greenstone, Zimbabwe: implications for provenance and source area weathering. *Geochim et Cosmochim Acta*, 60: 1751-1763.

Fedo, C.M., Young, G.M., Nesbitt, H.W. and Hanchar, J.M. (1997) Potassic and sodic metasomatism in the Southern Province of the Canadian Shield: Evidence from the Paleoproterozoic Serpent Formation, Huronian Supergroup, *Precambrian Research*, 84: 17-36.

Finkelman R. B., Dai S., French D. (2019). The importance of minerals in coal as the hosts of chemical elements: A review *International Journal of Coal Geology* 212, 1-17

Gill, S., Yemane, K (1996). Implications of a lower Pennsylvanian Ultisol for equatorial Pangean climates and early, oligotrophic, forest ecosystems. *Geology*, 24(10): 905-908.

Goldberg, E.D., Arrhenius, G.O.S., (1958). Chemistry of Pacific pelagic sediments, *Geochim. Cosmochim. Acta* 13, 153–212.

Gu, X.X., Liu, J.M., Zheng, M.H., Tang, J.X., and Qt, L. (2002). Provenance and Tectonic settings of the Proterozoic turbidites in Hunan, South China: Geochemical Evidence: *Journal of Sedimentary Research*, 72, 393– 407, 2002

Hatch, J.R., Leventhal, J.S. (1992). Relationship between inferred redox potential of the depositional environment and geochemistry of the Upper Pennsylvanian (Missourian) Stark Shale Member of the Dennis Limestone, Wabaunsee County, Kansas, USA. *Geology*, 99, 65 –82

Hu, W.Y.; Huang, B.; He, Y.; Yusef, K.K. (2016). Assessment of potential health risk of heavy metals in soils from a rapidly developing region of China. *Hum. Ecol. Risk Assess*. 22, 211– 225.

Johnsson, M.J. and Basu, A. (1993). Processes Controlling the Composition of Clastic Sediments. *Geological Society of America*, 284(Special Paper): .342.

Jones, B., Manning, D.A.C. (1994). Comparison of geochemical indices used for the interpretation of palaeoredox conditions in ancient mudstones. *Chemical Geology*, 111, 111–129.

Lelono E. B. (2017). Pleistocene climate of Indonesia, 6th International Conference on Earth Science and Climate Change.

Liang, Q., Tian, J., Zhang, X., Sun, X. and Yang, C. (2020). Elemental geochemical characteristics of Lower−Middle Permian mudstones in Taikang Uplift, southern North China Basin: implications for the FOUR-PALEO conditions. *Geosciences Journal*, 24(1), 17−33

McLennan, S.M., Taylor, S.R. (1985). Sedimentary rocks and crustal evolution: Tectonic setting and secular trends. *Journal of Geology*, 99: 1-21.

Michael E. B., ,Alan G. S., .Jeremy C. W., Wendy S. W., Robyn H., Ghulam M. B. (2019). Palaeoenvironments and elemental geochemistry across the marine Permo-Triassic boundary section, Guryul Ravine (Kashmir, India) and a comparison with other North Indian passive margin sections. *The Depositional Record*, 6 (1), 75-116

Nesbitt, H.W., Young, G.M., McLennan, S.M. and Keays, R.R. (1996). Effect of chemical weathering and sorting on the petrogenesis of siliciclastic sediments, with implications for provenance studies. *Journal of Geology*, 104: 525–542.

Nugrahanto N, Scott W. McFall, Estella F. (2001). Submarine-Fan Deposition in The Lower Steenkool Formation, Bintuni Basin, Irian Jaya, Eastern Indonesia: "Deep Water Reservoir Potential?", *Indonesian Sedimentology Forum (FOSI)*, 2nd Regional Seminar: 1-7.

Nussman, D.G., (1965). Trace Elements in the Sediments of Lake Superior. Unpubl. PhD thesis. University of Michigan, Ann Arbor (243 p).

Putra, A. and Husein, S. (2019). Regional overview of orogenic belts in Indonesia: emphasis on the occurrences of thrust wedge systems, *Berita Sedimentologi*, 44, 19-43

Pieters, P. E., A. Sufni Hakim, dan S. Atmawinata, (1990), Geologi Lembar Ransiki, Irian Jaya, Skala 1 : 250.000, Bandung: Pusat Penelitian dan Pengembangan Geologi

Potter P.E., Maynard J. B., and W. A. Pryor. (1980). Sedimentology of shale, Springer-Verlag

Retallack G. (2020). Boron paleosalinity proxy for deeply buried Paleozoic and Ediacaran fossils, *Palaeogeography, Palaeoclimatology, Palaeoecology* , 540, 1-13.

Rimmer S. M. (2004). Geochemical Paleoredox Indicators in Devonian-Mississippian Black Shales, Central Appalachian Basin (USA). *Chemical Geology*, 206, 373-391.

Rosser, B. P. and Korsch, R. J. (1988). Provenance signature of sandstone mudstone suite determined using discriminant function analysis of major element data. *Chemical Geology* l., 67: 119-139

Ross, D.J.K and Bustin, R.M. (2009). Investigating the use of sedimentary geochemical proxies for paleoenvironment interpretation of thermally mature organic-rich strata: Examples from the Devonian-Mississippian shales, Western Canadian Sedimentary Basin. *Chemical Geology*, 260, 1–19.

Sapiie, B., (2012). Geology and tectonic evolution of Bird Head Region Papua, Indonesia: Implication for Hydrocarbon Exploration in the Eastern Indonesia, AAPG International Convention and Exhibition.

Seppala M., Palsas and related forms. – In: Clark, M.J. (ed.): Advances in periglacial geomorphology: 247-278, John Wiley, Chichester., 1988

Sheldon, N.D., Retallack, G.J. & Tanaka, S. (2002). Geochemical climofunctions from North American soils and application to palaeosols across the Eocene-Oligocene boundary in Oregon. *Journal of Geology*, 110, 687–696.

Sheldon, N.D. (2006). Quaternary glacial-interglacial climate cycles in Hawaii. *Journal of Geology*, 114, 367–376.

Taylor and McLennan, (1985), The continental crust: Its composition and evolution, Blackwell, Oxford: 312, 1985

Xi, D.P., Wan, X.Q., Jansa, L., Zhang, Y.Y. (2011). Late Cretaceous palaeoenvironment and lake level fluctuation in the Songliao Basin, northeastern China. *Island Arc* 20, 6-22.

Xiaochun Z, Cunlei Li, Jinliang Z, Guiyang and Panpan Chen. (2020), Geochemical characteristics and depositional environment of the Shahejie Formation in the Binnan Oilfield, China, *Journal of Geophysics and Engineering* , 539–551